

Hongwu Wang, MD, PhD
 Peter J. Littrup, MD
 Yunyou Duan, MD
 Yanqun Zhang, MD
 Huasong Feng, MD
 Zhoushan Nie, MD

Published online
 10.1148/radiol.2351030747
 Radiology 2005; 235:289–298

Abbreviations:

KPS = Karnofsky Performance Scale
 PCT = percutaneous cryotherapy

¹ From the Tumor Targeted Cryotherapy Center, PLA General Navy Hospital, Beijing, China (H.W., Y.D., Y.Z., H.F., Z.N.); and Department of Radiology, Wayne State University School of Medicine, Detroit, Mich (P.J.L.). Received May 12, 2003; revision requested July 21; final revision received May 7, 2004; accepted June 28. **Address correspondence to** P.J.L., Department of Radiology, Harper University Hospital, 3990 John R St, Detroit, MI 48201 (e-mail: littrup@karmanos.org).

Authors stated no financial relationship to disclose.

Author contributions:

Guarantors of integrity of entire study, H.W., P.J.L.; study concepts and design, H.W., P.J.L., Y.D.; literature research, P.J.L.; clinical studies, H.W., Y.Z., H.F., Z.N.; data acquisition, H.W., Y.Z., H.F., Z.N.; data analysis/interpretation, H.W., P.J.L.; statistical analysis, H.W., P.J.L.; manuscript preparation, definition of intellectual content, editing, revision/review, and final version approval, P.J.L., H.W.

© RSNA, 2005

Thoracic Masses Treated with Percutaneous Cryotherapy: Initial Experience with More than 200 Procedures¹

PURPOSE: To perform and report initial experience with percutaneous cryotherapy (PCT) of the thorax.

MATERIALS AND METHODS: A human investigation committee approved the study protocol, and all patients gave informed consent. One hundred eighty-seven patients who were not surgical candidates underwent computed tomography (CT)-guided PCT for treatment of thoracic cancer masses. CT-visualized low-attenuating ice formation after PCT was compared with initial tumor size and location. At 1 week and at 1, 3, 6, and 12 months after PCT, the various findings seen on available CT scans and any complications were noted. χ^2 and Student *t* tests were used to identify significant differences in frequencies and mean values of imaging observations, respectively.

RESULTS: Ice formation was identified at CT as reduced attenuation values (in Hounsfield units) within soft-tissue masses, the mean sizes of which were 4.3 cm \pm 0.2 (standard deviation) in peripheral locations and 6.4 cm \pm 0.3 in central locations. Tumor size and location were independent predictors of tumor coverage by low-attenuating ice: Mean coverage was 99% for peripheral masses 4 cm or smaller (*n* = 101) and 80% for central masses larger than 4 cm (*n* = 58) (*P* < .001). An area of necrotic cavitation larger than the original mass developed in 80% (77 of 96) of masses within 1 week and was nearly resolved by 3 months in 7% (five of 76) of masses. By 6 months, minimal pulmonary scarring was noted in 56 patients and 86% of masses showed reduced or stable size. The overall rate of pneumothorax was only 12% (22 of 187 patients), and other side effects appeared to be self limited. No major bleeding or bronchial damage was noted. Two deaths in debilitated patients were temporally related, and two complications involved brachial and recurrent laryngeal nerve damage. The patient with laryngeal nerve damage regained speech within 2 months.

CONCLUSION: CT-guided PCT yielded low procedural morbidity given the extent of freezing, even near mediastinal structures. Ongoing advances in cryotechnology, imaging guidance, and treatment planning may help to avoid the degree of undertreatment of larger central masses observed in this study.

© RSNA, 2005

Many radiologists regard cryotherapy as an intraoperative modality that is used mainly by urologists and general surgeons for prostate gland and liver tumor ablations, respectively (1,2). For a long time, however, cryotherapy performed by using rigid bronchoscopes has been used extensively to treat endobronchial neoplasms and has yielded minimal morbidity (3–5). Outpatient acceptance of cryotherapy performed with flexible cryoprobes, lower cryotherapy equipment costs, and no bronchial perforation, as compared with the bronchial damage associated with the use of lasers (ie, for Nd:YAG or photodynamic therapy), have been noted by European investigators (6). Endobronchial cryotherapy has been considered the treatment of choice for early superficial bronchial carcinoma (7). The unique safety feature of cryotherapy—that of enabling preservation of the collagenous architecture (8)—and the resultant

integrity of the tracheobronchial tree (3–7) have appeared to be all but forgotten since heat-based therapies became more popular for percutaneous procedures.

The use of percutaneous tumor ablation has rapidly advanced, and radiofrequency is commonly used at many organ sites for applications that include treatment of primary lung cancer (9) and metastases originating from renal cell carcinoma (10). Experience with radiofrequency treatments remains in the early stages, but suggested drawbacks include heightened pain near the pleura and the chest wall; necrotic fistula formation—with potentially protracted pneumothoraces—caused by ablation near bronchi, and brisk scarring (cicatriziation) seen at longer-term follow-up (11). Thus, for central tumors, any heat-based therapy may have limited effectiveness owing to bronchial disruption or perforation from denatured protein. Imaging performed in a large population treated with percutaneous cryotherapy (PCT) is needed to define the general appearance of the treated area and to determine the feasibility of the procedure, particularly for the treatment of central neoplasms, including those with associated superior vena cava syndrome.

There has been a resurgence of the use of PCT for the treatment of prostate cancer in the urology community, primarily because of the improved ease of use of the procedure and reported long-term tumor control rates that are comparable to those achieved with surgery and radiation therapy (1). After the feasibility and excellent computed tomographic (CT) visualization of low-attenuating ice coverage of masses in pig livers (12) were documented, a group of interventionists (including P.J.L.) in collaboration with Chinese investigators performed percutaneous hepatic cryotherapy in humans in October 1999. China also has a burgeoning population of individuals with lung cancer, which leads to approximately 300 000 deaths per year in that country (13). Interventionists in China rapidly began performing PCT of the thorax after the U.S. experience with CT-guided PCT in September 2000 (14). The purpose of our study was to report our initial experience with PCT of the thorax.

MATERIALS AND METHODS

Patients

A human use protocol was approved by the senior medical oversight board (ie, human investigation committee) of PLA General Navy Hospital. An informed consent

TABLE 1
Histologic Distribution of Primary Tumors and Metastases

Cancer Type	No. of Patients	No. of Lesions
Primary tumor		
Squamous	74 (40)	77 (33)
Adenocarcinoma	72 (38)	96 (41)
Small cell	13 (7)	17 (7)
Unknown	6 (3)	6 (3)
Total	165 (88)	196 (84)
Metastasis		
Lung*	10 (5)	14 (6)
Colorectal	3 (2)	4 (2)
Kidney	1 (.5)	2 (1)
Hepatoma	1 (.5)	2 (1)
Osteosarcoma	2 (1)	6 (3)
Breast	1 (.5)	4 (2)
Nasopharyngeal	1 (.5)	3 (1)
Esophageal	1 (.5)	1 (.4)
Thyroid	1 (.5)	1 (.4)
Brain	1 (.5)	1 (.4)
Total	22 (12)	38 (16)

Note.—Numbers in parentheses are percentages based on a total of 187 patients or 234 lesions.
* Metastasis to lung identified postoperatively.

form was signed by all patients. The included patients primarily were considered to be ineligible for surgery, or they had undergone other lung cancer therapies that were unsuccessful. These patients fulfilled at least one of the following inclusion criteria: They had (a) single or multiple peripheral lung masses larger than 1.0 cm in diameter, with previous therapies (ie, radiation therapy, chemotherapy, and/or surgery) having failed; (b) a nonresectable (as determined, by means of surgical consultation, according to either tumor size and stage or health status) central lung cancer; (c) fewer than four metastases to the lung with controlled primary cancer; (d) a mass or adenopathy involving the mediastinum and/or the pericardium without distant metastases; and/or (e) malignant pleural effusion, which was considered as inclusion criteria only when it was associated with a distinct measurable primary lung tumor.

Exclusion criteria were as follows: five or more diffuse or bilateral masses; diffuse pleural metastases with a large effusion and no measurable primary mass; central masses to which percutaneous access was difficult (eg, associated with potential puncture of the major vasculature en route to a mass); severe pulmonary dysfunction associated with a maximum voluntary ventilation capacity lower than 39% (ie, a relative estimate of ventilatory capacity within 1 minute compared with the time frame for the predicted capacity; this parameter was used in lieu of the common measurement of a forced expiratory volume in 1 second of less than 1 L because it also yielded some insight with regard to

the musculoskeletal respiratory capacity and the degree of patient cooperation), the inability to lie flat, or respiratory distress at rest; severe cough, current respiratory distress, and/or difficulty to cooperate; and/or any bleeding dyscrasias that were not easily corrected.

One hundred eighty-seven patients with 234 masses underwent 217 PCT sessions as inpatients between August 2001 and September 2002 (Table 1). Male patients ($n = 137$) were predominant in this series. The mean age of all patients was 61 years (range, 41–83 years). Primary lung cancer accounted for 84% (196 of 234) of the masses and 88% (165 of 187) of the patients. Tumor stage was based on CT appearance alone, as determined by the primary treating radiologists (Y.Z., H.F., Z.N.) in conjunction with the staff oncologic pulmonologists (H.W., Y.D.). Of the 165 patients with primary lung cancer, five had stage I; 17, stage II; 20, stage IIIA; 60, stage IIIB; and 63, stage IV cancer. Of the patients with advanced stage disease (ie, stage III–IV), 89% (127 of 143) had already undergone surgery, chemotherapy, or radiation therapy. One hundred seventy-eight (76%) masses were treated during single cryotherapy sessions. Patients underwent repeated ablations for treatment of larger central masses or multiple pulmonary masses. For bilateral masses, repeated ablations were performed during separate sessions, whereas for multiple masses in the same lung, repeated ablations were performed simultaneously, when possible.



Figure 1. Three major steps to performing thoracic PCT in the current study. Left: First, needles (arrows) are placed in the tumor with CT guidance, and the hub is removed. Middle: The dilator-sheath combination (arrows) is placed, and its position is checked on CT images. Right: The cryoprobes (arrows) are then blindly placed to predetermined tumor depths, and the freeze cycle is begun: 20 minutes of freezing, 10 minutes of thawing, and then 20 minutes of refreezing.

PCT with CT Guidance and Calculated Cryoprobe Placement

All PCT procedures were performed by using an Elscint CT Twin II unit (Elscint, Haifa, Israel). Tumor location and size were noted at preoperative evaluation. A tumor was considered to be a central mass if it abutted any of the mediastinal or hilar structures. Tumor measurements were obtained in two dimensions on CT images, at the level of the tumor's most prominent appearance in the transverse plane. Patients were placed feet first into the CT gantry to allow easier access for subsequent needle and cryoprobe placements. CT fluoroscopy was not performed. Therefore, the procedures involved direct axial placement for optimal needle course visualization. Most patients received only local anesthetic agents and no sedatives. Those patients who were sedated received only a mild sedative (morphine 2–4 mg with or without midazolam hydrochloride 1–2 mg). Two interventional radiologists (P.J.L., Y.Z.) with many years of experience performing percutaneous biopsy and more than 10 years of experience performing clinical cryotherapy in other organ systems (P.J.L.) worked in conjunction with oncologic pulmonologists (H.W., Y.D.).

At the time of this study, only straight-shafted 3-mm-diameter cryoprobes were

available, and they were placed by using the technique shown in Figure 1. In addition, direct axial cryoprobe placements precluded the CT gantry clearance of the straight cryoprobes; thus, no CT imaging was performed during freezing. After the tumor was localized, the treatment area was prepared and draped in a sterile manner. Two percent lidocaine was injected into the pleural surface. To minimize the number of cryoprobe punctures, single-needle placement through the tumor center was chosen for smaller masses (ie, those 4 cm or smaller). A 19-gauge needle specially adapted by the lead author (H.W.) to be 20 cm in length and to have a removable hub but no inner stylet was used. The needle tip was placed through the mass to the far margin; then the hub was removed. We carefully noted the precise measurement of the final needle depth to determine the depth needed for subsequent sheath and cryoprobe placements.

The dilator and 11-F sheath were then slid over the needle to the depth of the needle insertion. The needle and dilator were removed, leaving the sheath in place to receive the 3-mm cryoprobe (Fig 1). The cryoprobe was blindly placed to the same predetermined depth at the far tumor margin since CT scanning could not be performed during freezing because

of the straight cryoprobe handles. The sheath was then retracted approximately 4 cm to expose the length at the tip of the cryoprobe that generates ice. If a substantial pneumothorax—that is, one greater than 2 cm in radial depth—was encountered during initial needle placement, a small (8-F) catheter was used for evacuation during PCT. If no persistent pneumothorax was seen, the catheter was removed at the end of PCT.

The cryotherapy equipment that we used consisted of an argon:helium gas-based system (CryoCare; Endocare, Irvine, Calif) and 2- and 3-mm-diameter cryoprobes (Endocare). With use of these cryoprobes, the diameters of the resulting ice balls may vary according to tissue type and blood supply, but the freeze lengths are consistent for both probes: approximately 4.5 cm. Ice ball diameter refers to the outer 0°C margin of the visible low-attenuating ice, but cytotoxic ice temperatures ($\leq 20^{\circ}\text{C}$) are known to occur 3–5 mm inside of visualized ice margins (1,2,8). For soft tissues (eg, liver and kidney), the estimated cytotoxic ice diameters that can be achieved by using 2- and 3-mm cryoprobes are 2.0 and 2.5 cm, respectively. Two-millimeter-diameter cryoprobes have a sharp tip and were used only when a direct-stick approach was chosen instead of the Seldinger approach described ear-

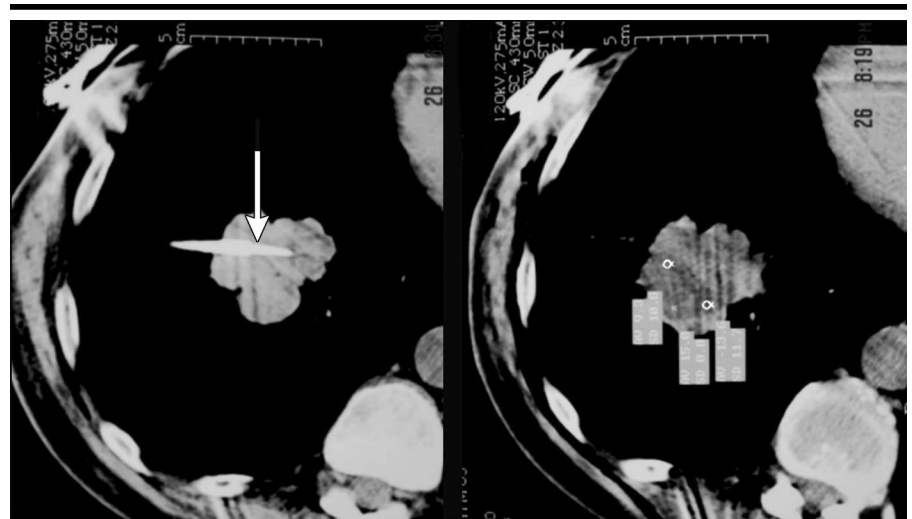
lier. Aerated lung parenchyma may serve as an insulator and thus lead to larger ice balls compared with those in soft tissues.

Since no animal model with comparably large lung tumors exists, the following assumptions were made after observing the low-attenuating ice that formed after PCT in the first several patients: For a mass within lung tissue, a 2-mm cryoprobe may produce an ice ball up to 3 cm in diameter, whereas a 3-mm cryoprobe may produce an ice ball up to 4 cm in diameter. Tumors 4 cm or smaller were treated by using one 3-mm cryoprobe. To avoid perfusion-mediated heating, we made no attempt to place additional cryoprobes for treatment of central masses.

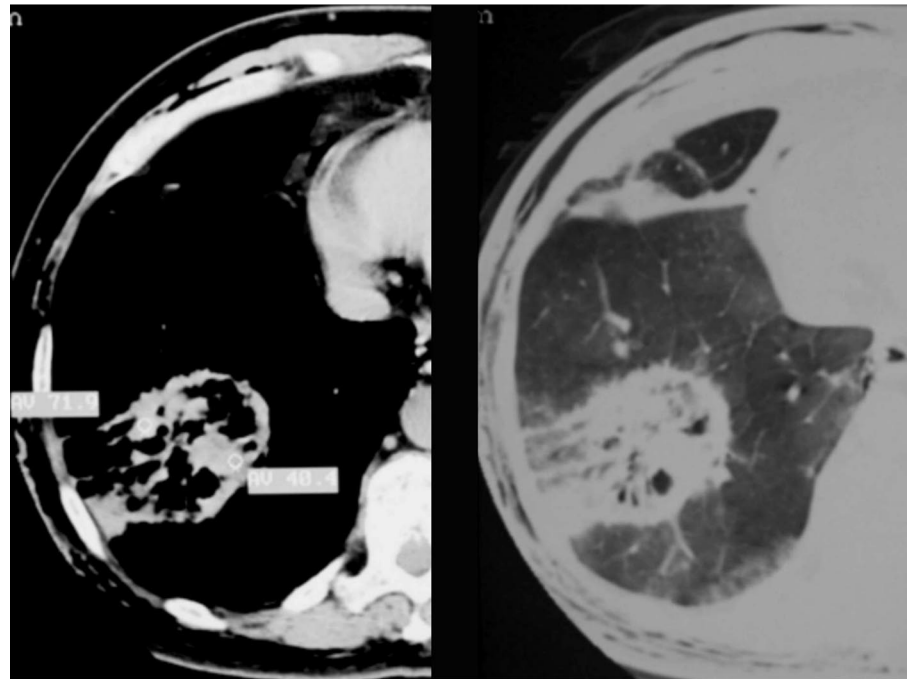
For this study, maximal freeze and thaw times were chosen to produce the largest feasible ice volume and ablation zone with the available cryoprobes, especially since imaging could not be performed during the procedure. To minimize pulmonary punctures, no thermocouples were used to monitor the temperature near tumor margins (similar to protocol used to treat prostate masses [1]). A treatment cycle consisted of a 20-minute freezing followed by a 10-minute thawing and then a 20-minute refreezing. The thaw cycle was defined as the cycle during which the temperature within the cryoprobe (ie, obtained from a thermocouple within the cryoprobe and approximating central ice ball temperatures) was allowed to increase either to 0°–5°C or until 10 minutes passed. With this protocol, we attempted to ensure maximal thawing of the ice ball and cytotoxicity of the ablation zone due to osmotic shock at the treatment margins. This thorough thawing phase is different from commonly used thawing phases (1,2) in which cryoprobes are not allowed to become mobile because their temperatures are kept lower than –4°C. With use of the “stick” mode on the cryoprobe system, one sets the thermostat to briefly activate the argon gas flow and thereby prevents cryoprobe movement. With our protocol, at the end of the second 20-minute freezing, the cryoprobes are allowed to undergo active thawing whereby helium is circulated through the cryoprobes. Owing to the isenthalpic properties of helium (ie, low molecular weight and low latent heat from vaporization), the cryoprobes are gently heated so that they can be removed within 2 minutes.

Postprocedural Evaluation and CT

Immediately after cryoprobe removal, the patient could fit back into the CT gantry for scanning and measurement of



a.



b.

Figure 2. CT image findings of immediate and short-term cryotherapy-induced cavitation. (a) Left: Slightly oblique transverse image obtained during PCT shows needle placement (arrow) in a 3-cm lobulated primary lung cancer. Right: Corresponding image obtained immediately after freezing shows low-attenuating ice throughout the mass. The boxes posterior to the tumor contain attenuation measurements (in Hounsfield units) that confirm the subzero temperature (ie, tissue ice formation) within the small circular regions of interest in the tumor. (b) Transverse soft-tissue (left) and lung window (right) CT images obtained 4 days after PCT show a well-circumscribed cavitory region covering the area of frozen tumor and the adjacent rim of pulmonary parenchyma seen in a. The treatment area appears to be more posterior now because the patient is no longer oblique but rather is lying supine.

low-attenuating ice formation. All CT scans obtained after PCT were acquired within the 2–3 minutes following the termination of freezing; during this time, the visible ice size remains relatively unchanged (1,2,8). It takes approximately 2 hours of CT time to perform most PCT

procedures, including cryoprobe placement and removal. CT attenuation values ranging from 0 to –10 HU were used to confirm solid ice formation. To estimate the percentage of any area of unfrozen tumor rim, bidimensional ice margin measurements were multiplied to pro-

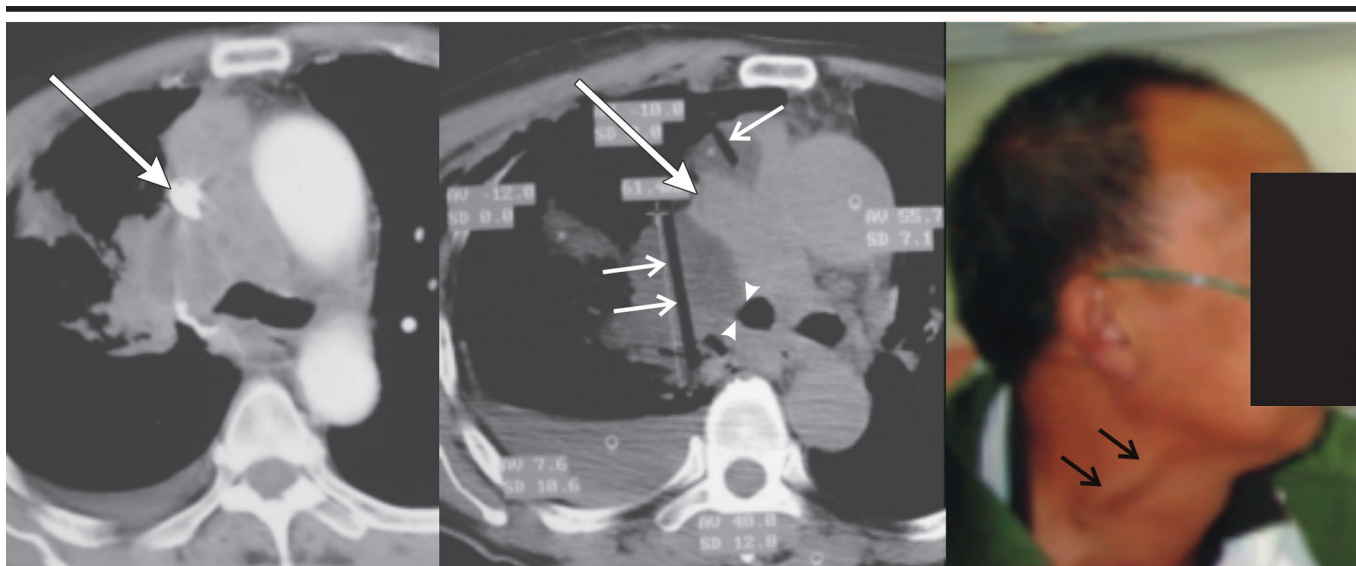


Figure 4. Transverse CT images obtained during cryotherapy for treatment of superior vena cava syndrome with use of multiple cryoprobes and during short-term clinical follow-up in patient who presented with facial edema and prominent jugular venous distention. Because of the lack of readily available emergent radiation therapy in China, this patient was treated for symptomatic relief via the immediate (2–3-day) cryotherapeutic “softening” that a tumor undergoes after ablation. Left: Contrast-enhanced image shows the superior vena cava (arrow) being displaced and compressed by bulky mediastinal and right hilar adenopathies. Middle: Nonenhanced image obtained immediately after cryoprobe removal shows the superior vena cava (large arrow) bracketed by low-attenuating ice, with air in the central cryoprobe tracks (small arrows). The low-attenuating ice extended into the right main bronchus (arrowheads) without complications. Right: Photograph of patient 3 days after PCT shows only mildly dilated neck veins (arrows) and resolved facial edema.

tion, 30–50 HU). However, the marked low attenuation (approximately –800 HU) of the adjacent aerated lung parenchyma made it impossible to visualize frozen tissue in the adjacent lung immediately after the freezing despite multiple window and level adjustments. Therefore, we could not document the desired visualization of extended areas of freezing (ie, 5–10 mm beyond the tumor mass) as can be done for other organs; rather, we documented only estimates of ice coverage of the soft-tissue components of the thoracic masses.

In an attempt to quantify initial treatment success, the estimated coverage of tumor areas by lower attenuating ice, as calculated by using bidimensional measurements, is summarized in Table 2. Tumor size and location were highly significant independent variables for determining the likelihood of tumor coverage by ice ($P < .001$). Tumor stage and type did not correlate with ice coverage once size and location were considered. The percentages of masses for which follow-up CT data collected over time were available are listed according to degrees of cavitation and changes in treated tumor size in Table 3. An area of cavitation larger than the original tumor was seen in 80% of treated areas 1 week after PCT (Fig 3, Table 3); a similar degree of necrotic cavitation has been

previously noted in patients with liver masses (2). The cavitation rate had decreased to only 7% (five of 76 treated areas) by 3 months, suggesting resorption of nearly all necrotic debris. By 6 months, 86% (48 of 56) of the treated areas were stable or smaller than the original tumor.

Complications and Early Follow-up Data

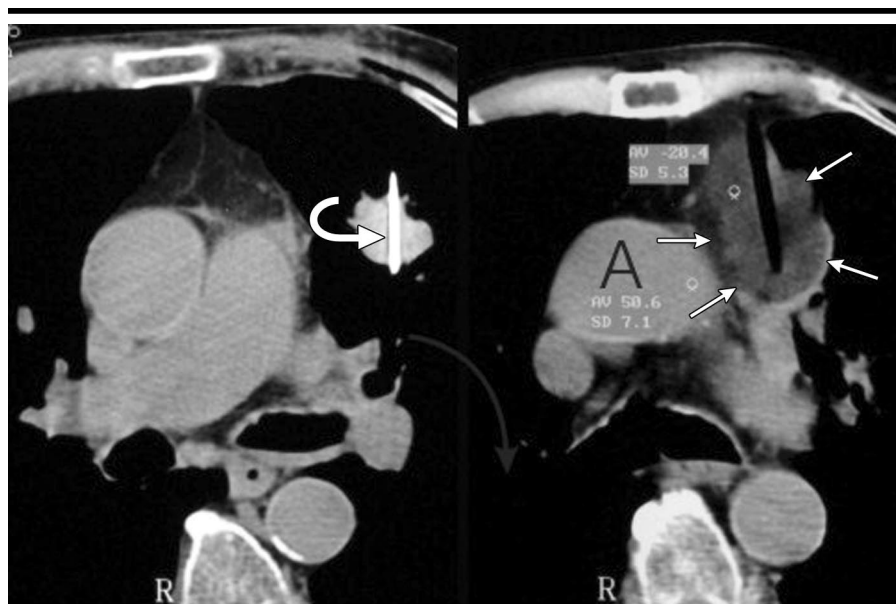
The complication rates listed in Table 4 emphasize a low pneumothorax rate and a predominance of self-limited (ie, lasting fewer than 5 days) side effects, despite major central freezing. No intraprocedural deaths were noted, but two deaths were temporally related: One patient died of a pulmonary embolus 1 day after cryotherapy, and the other died of acute respiratory distress syndrome a week later. However, no technical difficulties or other complications occurred during the procedure for either of these patients. Although follow-up data were too limited for the calculation of accurate survival estimates, the palliative benefits of PCT in terms of KPS performance status and general health status (eg, increased dietary intake and weight gain) were noted. In the group of 143 patients with advanced-stage cancer, general health and KPS statuses improved significantly 1

week after cryotherapy: The mean KPS score increased from 75.2 ± 1.3 before to 82.6 ± 1.4 1 week after PCT (Student $t = 3.87$, $P < .01$).

DISCUSSION

The short follow-up period for this large series of patients who underwent thoracic PCT precluded the calculation of reliable estimates of the effectiveness of this therapy for treatment of primary and metastatic lung tumors. That said, the long history of effective cryotherapy performed at other organ sites (1,2) makes the results obtained in this series encouraging in terms of at least patient safety and the feasibility of PCT for many thoracic locations. The observation that the minimal sedation used during PCT was well accepted by conscious patients suggests that PCT may become a treatment option for patients for whom general anesthesia poses risks, as well as those who are not surgical candidates. Several clinical assumptions and technical shortcomings need to be clarified since both cryotherapy equipment and imaging techniques continue to advance.

The diversity and large number of patients who underwent PCT in this study generate confidence in the technical aspects of thoracic tissue responses to cryo-



a.



b.

Figure 5. Transverse CT image findings of cryotherapy for treatment of pulmonary mass and associated anterior mediastinal adenopathy in a patient in whom chemotherapy was unsuccessful. (a) Images show needle placement in left upper lobe nodule (curved arrow) and final extent of ice coverage (straight arrows) in uppermost region of an anterior mediastinal mass abutting the ascending aorta (A). No complications were noted, but care was taken to avoid recurrent laryngeal nerve damage near the aortopulmonary window—that is, the freezing of this mass did not extend to the course of the nerve wrapping around the left main bronchus. (b) Left: Image shows small pretracheal nodes (curved arrows) at levels similar to those depicted in a on the right. Straight arrows mark ice coverage. Right: Image obtained at lower level shows ice extension (straight arrows) toward the aortopulmonary window but incomplete tumor coverage (curved arrow) where the posterior aspect of the tumor abuts the pulmonary artery (PA). The tumor was refrozen following regrowth, and local control was achieved for more than 1 year.

therapy. We acknowledge the potential bias in the selection of our patient groups and that cryotechnology was rapidly improving during the course of this study. The individuals treated with PCT were

mainly patients who were ineligible for surgery, and 89% (127 of 143) of them had advanced-stage cancer for which prior treatment had failed. Thus, the outcomes of these patients would be difficult

to compare because the PCT procedures were only palliative and were used for treatment of several tumor types. The large number of procedures, however, still enabled an accurate assessment of technique, and the results established the relative safety and feasibility of PCT for nearly all tumor locations.

The complementary effects of tumor size and tumor location on immediate postfreezing outcomes helped us redefine treatment goals and better generally plan cryotherapy procedures. Newly available angled cryoprobes allow much greater flexibility so that the degree of tumor undertreatment observed in this study, which occurred primarily because direct CT imaging could not be performed during cryoprobe placement and freezing, can be avoided.

Despite the limitations, thorough (99%) ice coverage was achieved by using a single 3-mm cryoprobe for 101 peripheral masses 4 cm or smaller. We now advocate bracketing small masses with single-puncture, 2.4-mm angled cryoprobes. By first placing a 20-gauge needle (eg, Westcott needle) near the center of the mass, one can directly place the larger cryoprobes with a trajectory parallel to the 20-gauge needle, allowing minimal repositioning and facilitating a lower risk of pneumothorax. However, central masses larger than 4 cm may require the most conservative cryoprobe distribution (eg, one cryoprobe for each 1.5–2.0-cm-diameter tumor) since in our study, only 80% coverage of these tumors was achieved. The intermediate categories of peripheral masses larger than 4 cm and central masses 4 cm or smaller also suggest the need for closer cryoprobe arrangements to maximize the freezing capacity per centimeter of tumor area (eg, one cryoprobe for each 2.5-cm diameter, similar to the placement protocol for other organs).

The ability to visualize lower attenuating ice as it thoroughly covers a soft-tissue tumor mass during the freeze cycles (12) is a potential benefit that is not available with heat-based treatments, which may require the use of special temperature-sensitive magnetic resonance imaging sequences that are performed by using limited-access open-bore units. CT imaging during freezing is crucial and can be performed with the straight-shafted cryoprobes that were used in this study, but it requires cranial angulation to avoid the gantry (ie, cranial probe angulation also helps to place cryoprobes in upper abdomen locations for percutaneous hepatic and renal approaches). In general, the greater the number of cryoprobes used, the larger the lethal ice zone

and the shorter the freeze time required to achieve thorough tumor coverage by low-attenuating ice. The suggested freeze times given in Figure 6 enable one to take advantage of the freezing capacity of the newer 2.4-mm-diameter L-shaped cryoprobes, which allow device insertion and procedural monitoring with CT fluoroscopy or spiral CT after each freeze, thaw, or refreeze cycle. The ability to place additional cryoprobes during the thaw cycle to cover any margins suspected of being undertreated also helps to alleviate any freezing variations related to tumor margins near major blood vessels or any freezing variations along an irregular outer margin. For these situations, we advocate the eccentric placement of cryoprobes closer to these vessels to intensify the freezing and avoid perfusion-mediated heating, without fear of vessel damage because the collagenous wall architecture of the vessels is preserved. However, great care should still be taken to avoid any vessel puncture by choosing the least vascular path discerned with lung window imaging settings.

Visualization of the treated area between freeze cycles allows additional cryoprobes to be placed during the thaw phase so that one can thoroughly cover a tumor during one session rather than blindly hope that empiric estimates of ice sizes in different tissues will still include all tumor margins. CT fluoroscopy during PCT now enables rapid and accurate placement of multiple cryoprobes, as well as intermittent monitoring of freeze extent. However, careful assessment of the freeze extent during the procedure is best achieved by performing limited spiral CT at the end of both freeze cycles (Figs 3a, 5b, 6) because use of the lower x-ray beam milliamperage setting in the CT fluoroscopy mode reduces spatial resolution and tissue contrast (ie, greater quantum mottle). Another immediate modification involves the use of the stick mode (at approximately -10°C) setting on the cryotherapy unit during the thaw cycle to prevent any cryoprobe movement—and associated inaccuracies—between freezes.

An area of cavitation larger than an original peripheral tumor indicates thorough ablation coverage (2,12,15) and should not be mistaken for an abscess, which would have air and fluid levels and thicker, enhancing rims. None of the study patients had clinical signs or symptoms of abscess or sepsis, and 80% (77 of 96) of lesions resolved asymptotically within a month. An area of cavitation larger than the original tumor is a good

TABLE 2
Tumor Location, Size, and Cryotherapy Coverage

Tumor Location and Diameter (cm)	No. of Masses	Percentage Tumor Area Covered by Ice*
Peripheral		
≤ 4	101	98.7 ± 0.8
> 4	65	87.2 ± 1.6
Central		
≤ 4	10	89.5 ± 3.8
> 4	58	79.6 ± 2.3

* Relative area ratios of low-attenuating ice compared with soft tumor tissue, based on bidimensional measurements and separated according to tumor size and location. Values are expressed as percentages \pm standard deviations. They reflect the average cross-sectional area of a tumor covered by low-attenuating ice per group and indicate a highly significant decrease in tumor coverage by ice with increasing tumor size and/or central location. Undertreatment was more likely for larger central tumors. $P < .001$ for difference in values between masses 4 cm or smaller and those larger than 4 cm and for difference in values between the central and peripheral tumors.

TABLE 3
Tumor Cavitation and Treatment Size Over Time

Feature	1 Week	1 Month	3 Months	6 Months	12 Months
CT scans available	96	61	76	56	12
Tumor appearance					
Cavitation	77 (80)	16 (26)	5 (7)	1 (2)	0 (0)
Enlargement	87 (91)	12 (20)	4 (5)	6 (11)	2 (17)
Size unchanged	8 (8)	14 (23)	18 (24)	23 (41)	4 (33)
$>50\%$ Involution	1 (1)	35 (57)	47 (62)	25 (45)	4 (33)
Disappeared	0 (0)	0 (0)	7 (9)	2 (4)	2 (17)

Note.—Data are numbers of treated masses. Numbers in parentheses are percentages based on the number of masses for which there were available scans at the given time point. The number of masses for which there were available scans became limited over time, but the images showed clear trends in terms of two separate imaging features over time: cavitation and size of treatment area. Cavitation nearly resolved by 3 months. Note that cavitation time course correlated well with treatment site enlargement, reflecting initial tissue destruction beyond the tumor and then involution or stability of the treatment site by 6 months in 86% of cases.

outcome that emphasizes the need for approximately 1-cm ablative margins as treatment goals. Cavitation surrounding all previous tumor margins also may serve as an indicator of thorough treatment effect, and in our study, 57% (35 of 61) of the treated areas were reduced by more than 50% at 1 month.

The CT appearances of the treated areas over time suggested that even in cases of visible undertreatment, gross tumor regrowth may not be seen until after 3 months. This observation is very similar to those described in reports of radiofrequency treatment: irregular enhancement requiring re-treatment within 3–6 months (16). Owing to the small sample size of cases with available follow-up data, it is currently premature to assess any differential responses between tumor types or to assess the findings in patients who potentially had tumor regrowth after incomplete treatment. The matching of the outcomes summarized in Table 2 with the observations presented in Table 3 will be addressed in future efficacy stud-

ies. Detailed positron emission tomography data in conjunction with thin-section contrast material-enhanced CT data may be required to define the short-term imaging parameters that can be used to better predict long-term clinical outcomes.

The 12% pneumothorax rate for PCT suggests the self-limited nature of cryotherapy-induced pneumothoraces, nearly half of which were simply evacuated during the procedure. Cryotherapy can preserve the collagenous architecture of virtually any frozen tissue (3–8), and, thus, it may facilitate the rapid natural closing of cryoprobe tracks. Data are limited for both ends of the temperature-related treatment spectrum, but radiofrequency cryoprobes could cauterize tissue channels and become more prone to causing persistent—or larger—pneumothoraces that progress to bronchopleural fistulas (11). Animal studies may be beneficial for assessing these possibilities, but again, such studies may be impractical because the tumor masses in the animals may not be of sufficient size for relevant

TABLE 4
Complications of PCT

Complication	No. of Procedures*	Comments†
Cough	171 (79)	Only five (3%) cases exaggerated after cryotherapy
Hemoptysis	134 (62)	Stopped within 1 week; no intervention (embolization) required
Fever	91 (42)	Slight or moderate (<38.5°C); resolved within 1–5 days with antiinflammatory medication
Hypertension	72 (33)	Self limited and mild to moderate; occurred only during lesion freezing
Pleural effusion	30 (14)	More frequent with pleura-based tumors; five (17%) effusions drained
Pneumothorax	26 (12)	Twelve (46%) cases required periprocedural evacuation, 11 (42%) cases clinically unimportant, three (12%) cases required catheter drainage for 5–7 days
Subcutaneous emphysema	11 (5)	Commonly occurred in elderly patients; absorbed in 3–5 days
Skin injury	10 (5)	Minimal at puncture site; easily prevented by using water-filled glove
Death	2 (1)	Neither intraprocedural; one case owing to ARDS and one case owing to pulmonary embolus
Arm paralysis	1 (.5)	Brachial plexus damage from direct approach
Loss of speech	1 (.5)	Temporary aphasia from recurrent laryngeal nerve damage
All	217 (100)	...

Note.—The more common complications were self-limited and did not require intervention or symptom treatment, whereas the more severe complications (eg, pneumothorax) were relatively uncommon given the extent and complexity of PCT in this series.

* Numbers in parentheses are percentages.
† ARDS = acute respiratory distress syndrome.

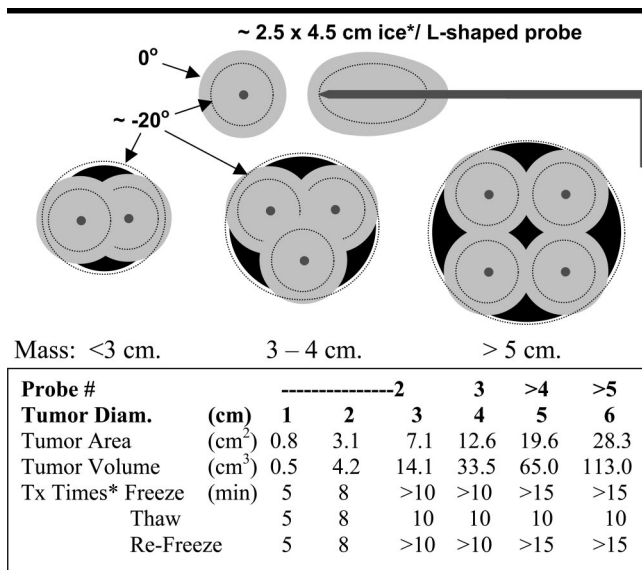


Figure 6. Illustration of current PCT equipment and outline of protocols for thorough freezing. The number of cryoprobes and the projected freeze schedules relate to tumor diameter. The dashed line inside the ice balls indicates increasing extent of lethal (eg, $\leq 20^{\circ}\text{C}$) ice coverage because more cryoprobes are used to cover the mass. The bracketing approach (ie, with use of two cryoprobes) for treatment of small (<3 cm) masses helps to eliminate operator dependency in the precise placement of cryoprobes in the center of the tumor and to extend cytotoxic margins, and it may facilitate shorter freezing times. Projected ice ball sizes vary according to the tumor's location near major vessels and the background tissue in which it resides (eg, lung, liver, kidney, or bone). *Diam.* = diameter, *Tx* = treatment.

their transient nature and the associated very low rate of progression to serious conditions that require treatment. Minor hemoptysis resolved within 1 week and did not require further intervention. The hypertension that occurred during active freezing, which accounted for 33% of the complications, was mild to moderate and self limited; however, the occurrence of this complication should be noted in patients who have preexisting hypertension and thus may require additional treatment adjustments. The nerve damage seen in two patients reinforces the need for careful planning of the treatment near the brachial plexus and supports concerns regarding recurrent laryngeal nerve damage when the freezing involves the aortopulmonary window. The return of speech in this patient is consistent with previous reports of potential nerve regeneration due to the sheath remaining intact (17), unlike the integrity of this structure following heat-based ablation or surgery. The two deaths appeared to be temporally related and suggest the need for caution and careful follow-up of patients with limited pulmonary reserve.

Cryotherapy can preserve the collagenous architecture of the central bronchi and the vasculature, as suggested by reported endobronchial cryotherapy experiences (3–8). The ability to perform tumor ablations immediately adjacent to central bronchi may represent a major difference between cryotherapy and heat-based treatments. New treatment opportunities for combined mediastinal therapies may exist, involving cryotherapy in conjunction with lower radiation doses (18–20) and/or chemotherapy (21,22). Thus, future treatments for advanced-stage lung cancers may have lower overall side effects (eg, minimal scarring) owing to the use of debulking combined with cryotherapy. In addition, the patients with advanced disease in this study felt better—that is, their KPS scores increased—within 1 week after undergoing cryotherapy. We are uncertain whether this outcome was simply a placebo effect or was related to tumor debulking and a resultant reduction in paraneoplastic effects. Thorough staging (ie, not just CT staging), improved ablation planning and monitoring, longer follow-up periods (eg, with CT, PET, and extended KPS scoring), and potential treatment combinations need to be addressed for future cryotherapy protocols.

The main limitation of this report is the lack of long-term follow-up data on the study patients, who predominantly were ineligible for surgery and had un-

comparisons with tumor masses in humans.

The other side effects and complications of PCT seen in this study reflect

dergone other treatments that failed. Therefore, this was not a definitive trial for assessing the effectiveness of PCT for treatment of either newly diagnosed primary cancers or metastatic lung tumors. Our report of the large number of procedures for which imaging findings were available should serve only as a thorough documentation of safety, feasibility, and technique considerations. Further PCT experiences with fluoroscopic CT guidance and monitoring performed by using the newer CT-compatible cryoprobes are needed to minimize or eliminate visibly undertreated areas of larger and central tumors, such as those seen in this study. We also suggest that interventionists engage in more standardized cryotherapy planning to better adapt to the continually improving cryotechnology and to mitigate operator-dependent outcomes. Despite some early technical shortcomings, the feasibility of achieving cryotherapeutic control of local tumor growth was safely demonstrated in the described large group of patients, who could not undergo surgery and/or had previously undergone frontline therapy that failed.

In summary, CT-guided PCT was associated with low procedural morbidity, even with freezing near mediastinal structures, which also appear to heal without substantial scarring or sequelae. Ongoing advances in cryotechnology and imaging guidance techniques may help interventionists avoid the degree of undertreatment of larger central masses observed in the current study and improve treatment planning.

References

1. Bahn DK, Lee F, Badalament R, Kumar A, Greski J, Chernick M. Targeted cryoabla-

- tion of the prostate: 7-year outcomes in the primary treatment of prostate cancer. *Urology* 2002; 60(2 suppl 1):3-11.
2. Lee FT, Mahvi DM, Chosy SG, et al. Hepatic cryosurgery with intraoperative US guidance. *Radiology* 1997; 202:624-632.
3. Sanderson DR, Neel HB, Fontana RS. Bronchoscopic cryotherapy. *Ann Otol Rhinol Laryngol* 1981; 90:354-358.
4. Homasson JP. Bronchoscopic cryotherapy. *J Bronchol* 1995; 2:145-153.
5. Maiwand MO. The role of cryosurgery in palliation of tracheo-bronchial carcinoma. *Eur J Cardiothorac Surg* 1999; 15:764-768.
6. Mathur PN, Wolf KM, Busk MF, Briete M, Datzman M. Fiberoptic bronchoscopic cryotherapy in the management of tracheobronchial obstruction. *Chest* 1996; 110:718-723.
7. Deygas N, Froudarakis, Ozenne G, Vergnon JM. Cryotherapy in early superficial bronchogenic carcinoma. *Chest* 2001; 120:26-31.
8. Littrup PJ, Mody A, Sparschu RA, et al. Prostatic cryotherapy: ultrasonographic and pathologic correlation in the canine model. *Urology* 1994; 44:175-184.
9. Dupuy DE, Zagoria RJ, Akerley W, Mayo-Smith WW, Kavanagh PV, Safran H. Percutaneous radiofrequency ablation of malignancies in the lung. *AJR Am J Roentgenol* 2000; 174:57-59.
10. Zagoria RJ, Chen MY, Kavanagh PV, Torti FM. Radio frequency ablation of lung metastases from renal cell carcinoma. *J Urol* 2001; 166:1827-1828.
11. Dupuy DE, Mayo-Smith WW, Abbott GF, DiPetrillo T. Clinical applications of radio-frequency tumor ablation in the thorax. *RadioGraphics* 2002; 22:S259-S269.
12. Lee FT Jr, Chosy SG, Littrup PJ, Warner TF, Kuhlman JE, Mahvi DM. CT-monitored percutaneous cryoablation in a pig liver model: pilot study. *Radiology* 1999; 211:687-692.
13. Liu BQ, Peto R, Chen ZM, et al. Emerging tobacco hazards in China. I. Retrospective proportional mortality study of one million deaths. *BMJ* 1998; 317:1411-1422.
14. Littrup PJ, Wang H, Duan Y, Zhang Y, Feng H, Nie Z. Percutaneous cryotherapy of the thorax: clinical observations from more than 200 procedures (abstr). *Radiology* 2003; 229(P):438.
15. Rodgers BM, Blake KD, Alexander JA. The effects of profound cryotherapy upon the pulmonary parenchyma. *J Thorac Cardiovasc Surg* 1982; 83:784-789.
16. Gervais DA, McGovern FJ, Arellano RS, McDougal WS, Mueller PR. Renal cell carcinoma: clinical experience and technical success with radio-frequency ablation of 42 tumors. *Radiology* 2003; 226:417-424.
17. Moorjani N, Zhao F, Tian Y, Liang C, Kaluba J, Maiwand MO. Effects of cryoanalgesia on post-thoracotomy pain and on the structure of intercostal nerves: a human prospective randomized trial and a histological study. *Eur J Cardiothorac Surg* 2001; 20:502-507.
18. Fukumoto S, Shirato H, Shimzu S, et al. Small-volume image-guided radiotherapy using hypofractionated, coplanar, and noncoplanar multiple fields for patients with inoperable stage I nonsmall cell lung carcinomas. *Cancer* 2002; 95:1546-1553.
19. Vergnon JM, Schmitt T, Alamartine E, Barthelemy JC, Fournel P, Emonot A. Initial combined cryotherapy and irradiation for unresectable non-small cell lung cancer: preliminary results. *Chest* 1992; 102:1436-1440.
20. Chen A, Galloway M, Landreneau R, et al. Intraoperative ¹²⁵I brachytherapy for high-risk stage I non-small cell lung carcinoma. *Int J Radiat Oncol Biol Phys* 1999; 44:1057-1063.
21. Homasson JP, Pecking A, Roden S, Angebault M, Bonniot JP. Tumor fixation of bleomycin labeled with 57 cobalt before and after cryotherapy of bronchial carcinoma. *Cryobiology* 1992; 29:543-548.
22. Clarke DM, Baust JM, Van Buskirk RG, Baust JG. Chemo-cryo combination therapy: an adjunctive model for the treatment of prostate cancer. *Cryobiology* 2001; 42:274-285.